

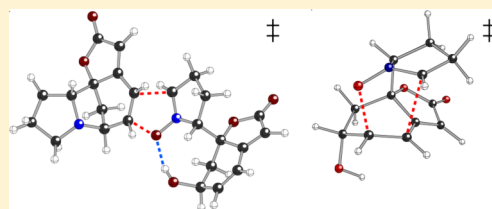
# The Viability of Nitron–Alkene (3 + 2) Cycloadditions in Alkaloid Biosynthesis

Phillip P. Painter, Ryan P. Pemberton, Bonnie M. Wong, Krystina C. Ho, and Dean J. Tantillo\*

Department of Chemistry, University of California, Davis, 1 Shields Avenue, Davis, California 95616, United States

**S** Supporting Information

**ABSTRACT:** Although evidence has mounted in recent years for the biosynthetic relevance of [4 + 2] cycloaddition reactions, other cycloadditions have received much less attention. Herein we used density functional theory (DFT) calculations to assess the viability of nitron–alkene (3 + 2) cycloaddition reactions proposed to occur during the biosynthesis of several alkaloid natural products (flueggines and virosaines). The results of our calculations indicate that these reactions have low enough intrinsic barriers and diastereoselectivity that they can proceed without enzymatic intervention.



While the possible involvement of [4 + 2] cycloadditions—both with and without enzymatic assistance—in biosynthetic pathways has received considerable notoriety,<sup>1–5</sup> biosynthetic dipolar cycloadditions have received much less attention. Among these, oxidopyriliun–alkene cycloadditions are perhaps best known, having been demonstrated to be feasible in total syntheses of terpenoid natural products<sup>6,7</sup> and having been shown by quantum-chemical calculations to have barriers of approximately 20 kcal/mol for biosynthetically relevant systems.<sup>8</sup> Herein we describe a quantum-chemical study of (3 + 2) nitron–alkene cycloadditions leading to complex alkaloid natural products. Our results indicate that enzymatic intervention is not necessary to lower the barriers or control the regio- and stereoselectivity of these transformations.

Flueggine A and the virosaine alkaloids (Scheme 1), all isolated from *Flueggea virosa*,<sup>9–12</sup> have very different molecular architectures, but all contain (in addition to their butenolide substructures) central isoxazolidine rings. It was proposed that these rings could be produced by biosynthetic nitron–alkene cycloadditions,<sup>11,12</sup> all involving diastereomers of the same precursor, **1** (Scheme 1). This precursor could be derived from oxidative cleavage of the known alkaloid norsecurinine or through an independent pathway from tyrosine. An intermolecular reaction with norsecurinine could produce flueggine A (Scheme 1, left), although it is not obvious whether the isomer found in nature would be inherently preferred. Intramolecular cycloaddition of particular stereoisomers of **1** would lead to virosaines A and B (Scheme 1, right). The viability of both types of cycloaddition in abiological environs (nonpolar organic solvents at elevated temperatures) was demonstrated by Yang, Li, and co-workers.<sup>13</sup> We now describe the results of density functional theory (DFT) calculations<sup>14</sup> on these reactions and discuss the predicted magnitudes of the barriers for nonassisted cycloaddition and the magnitude, direction, and origins of the inherent selectivity for these complex molecules.

**Toward Flueggine A.** First we consider flueggine A-forming cycloadditions. Because both the dipole and dipolarophile are chiral, eight different cycloaddition transition state arrangements are possible, differing in regiochemistry and stereochemistry (*endo* vs *exo* and attack from either face of the dipolarophile). These transition state structures were first located in the gas phase using a model system consisting of norsecurinine in its entirety but 2-methylnitron as a dipole. The lowest-energy computed transition state structure corresponded to the geometry that would produce the natural diastereomer of flueggine A. The three transition state structures with the next-lowest predicted energies were all approximately 4 kcal/mol higher in energy than the lowest. These four transition state geometries were then re-examined using **1** as a dipole. For all four, the dienone was oriented in such a way that its hydroxyl group could participate in hydrogen bonding with the nitron oxygen. The resulting transition state structures are shown in Figure 1. The preferred transition state structure for the full system is again that which would produce the natural diastereomer of flueggine A (Scheme 1). The predicted energy barrier for cycloaddition in water via this transition state structure is 10.3 kcal/mol (based on the energy of separated reactants); gas-phase calculations indicate that this barrier would be increased by 13–14 kcal/mol upon inclusion of entropy and thermal corrections. Distortion/interaction analysis<sup>24–28</sup> indicated that this transition state structure is preferred over the other three in Figure 1 because it has both a smaller distortion energy and a larger interaction energy (see the Supporting Information for details).

In that there is an inherent preference for the formation of flueggine A rather than alternative constitutional isomers or stereoisomers, it seems clear that selectivity control by an enzyme is not required. Nonetheless, this reaction could be

**Received:** November 8, 2013

**Published:** November 15, 2013

**Scheme 1. Biosynthetic and Biomimetic (3 + 2) Cycloadditions: Proposed (3 + 2) Cycloadditions in the Biosynthesis of Flueggine A and Virosaines A and B (Note That Different Diastereomers of 1 Lead to Different Classes of Natural Products)**

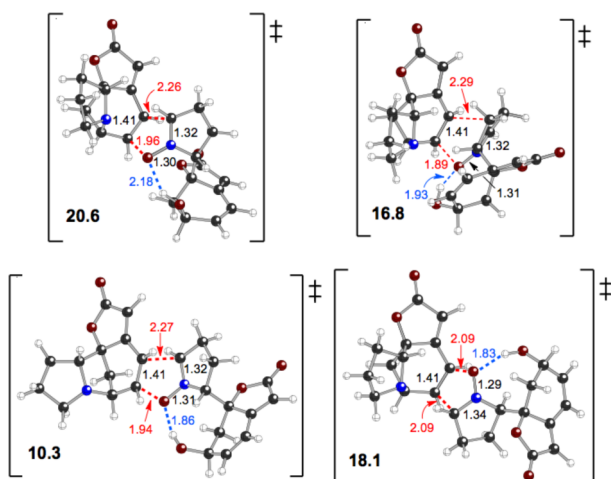
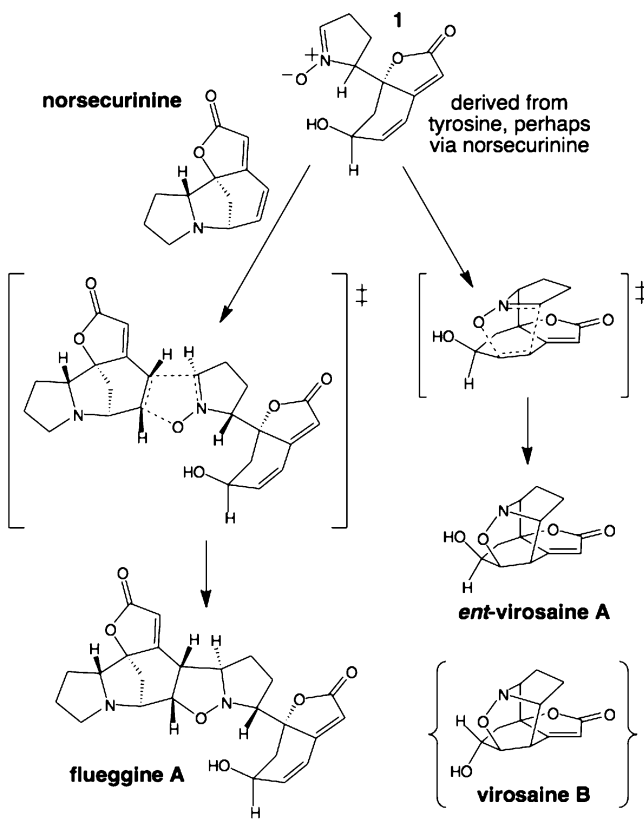


**Figure 1. Transition state structures—intermolecular:** computed transition state structures for cycloaddition of **1** with norsecurinine. Selected distances (Å) are shown; predicted energy barriers (kcal/mol) in water [SMD(water)-M06-2X/6-311++G(d,p)//M06-2X/6-31+G(d,p)] are shown in bold text.

promoted by bringing the two reactants together *without disrupting the inherent preference for product formation*. If **1** is indeed produced from norsecurinine (Scheme 1), the two reactants will be present in the same local environment.

The norsecurinine + **1** reaction was also carried out in toluene at elevated temperatures, and flueggine A was formed in 77%

yield under these conditions.<sup>13</sup> Our predicted barriers and selectivity for reaction in the gas phase would be expected to correlate with this experimental observation, and they do—the transition state structure leading to flueggine A is again predicted to predominate (by 2.2 kcal/mol over the next-lowest transition state structure), and a barrier of 22.9 kcal/mol for the cycloaddition is predicted.

**Toward the Virosaines.** In principle, diastereomers of nitron **1** could also undergo *intramolecular* (3 + 2) cycloadditions to produce the virosaines (Scheme 1 and Figure 2). Transition state structures for the formation of *ent*-virosaine

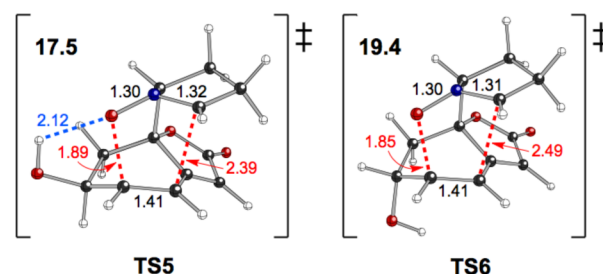


**Figure 2. Transition state structures—intramolecular:** computed transition state structures and predicted barriers [SMD(water)-M06-2X/6-311++G(d,p)//M06-2X/6-31+G(d,p)] for intramolecular cycloaddition of **1**. Selected distances (Å) and energy barriers (kcal/mol, in bold) are shown.

A and virosaine B are shown in Figure 2. The barriers for formation of the virosaines (based on the lowest-energy conformers of reactants) are predicted to be in the range where enzymatic intervention is not absolutely required (these barriers are predicted to increase by only ~1 kcal/mol upon inclusion of entropy and thermal corrections).

Distortion/interaction energy analyses of TS5 and TS6 were difficult to perform because the dipole and dipolarophile were part of the same molecule and connected by a very short tether.<sup>29</sup> Instead, two truncated versions of the dipolarophile were examined (Figure 3, top). Not surprisingly, a larger interaction energy was found for transition state structures with shorter forming C–O bonds. This effect appears to outweigh the effect of a corresponding lengthening of the forming C–C bond, indicating that the interaction energy is correlated to the asynchronicity in this case, which would serve to help the virosaine-forming reactions (note the forming bond lengths shown in Figure 2 and Figure 3, bottom). Dipolarophile distortion appears to be correlated in the opposite sense, however, partly counteracting this effect for the small model systems shown but likely overwhelming it for the highly constrained TS5 and TS6, which have barriers larger than those predicted for the small model systems.

The barriers for formation of virosaine B and *ent*-virosaine A are affected by several compensatory factors. During these processes, the allylic CHOH groups pucker away from the dipole; consequently, the  $\pi_{C=C} \leftrightarrow \sigma^*_{C-O}$  alignment decreases for the *ent*-virosaine A-forming reaction but increases for the virosaine B-forming reaction. A natural bond orbital (NBO) analysis<sup>30</sup> revealed a stabilization of 5.1 kcal/mol for donation of the  $\sigma_{C-O}$  orbital (of the forming bond) into the accepting  $\sigma^*_{C-O}$  orbital (of the OH group) of the transition state structure leading to virosaine B. This effect is largely counterbalanced, however, by a stabilization of 3.0 kcal/mol in the transition state structure leading to *ent*-virosaine A from donation of the

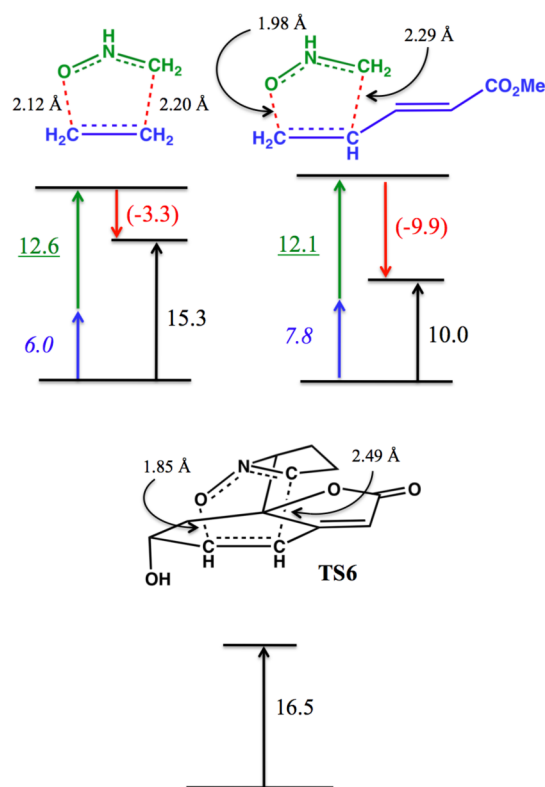


**Figure 3.** Distortion/interaction energy analysis of the transition state leading to virosaine B. Two truncated models are shown with dipolarophile distortion energies (italics, blue), dipole distortion energies (underlined, green), interaction energies (parentheses, red), and electronic energy barriers (plain, black, without zero-point energy correction). All energies [M06-2X/6-311++G(d,p)//M06-2X/6-31+G(d,p)] are in kcal/mol.

$\sigma_{C-H}$  orbital into the  $\sigma_{C-O}^*$  orbital (of the forming bond). The remaining energy difference is likely made up through differences in dipole distortion and other smaller interactions.

**Enzyme Intervention or Not?** Is enzyme intervention necessary for the flueggine- and virosaine-forming reactions to be biosynthetically feasible? The free energy barriers for cycloadditions leading to these natural products are predicted to be 20–24 kcal/mol. A free energy barrier of 23 kcal/mol corresponds to a half-life of approximately 1 h at room temperature, implying that enzymatic intervention is not absolutely required.<sup>8</sup> Although reducing the polarity of the environment and reducing the entropy penalty associated with cycloaddition will lower the barriers to some extent, the associated impediments to cycloaddition are not prohibitive. Consequently, we conclude that nitron–alkene cycloadditions are indeed viable steps in the biosynthesis of alkaloids.<sup>31</sup>

## ■ ASSOCIATED CONTENT

### Supporting Information

Full details of computational methods; additional details on computational results, including coordinates and energies for all computed structures; and complete citations of refs 16 and 23. This material is available free of charge via the Internet at <http://pubs.acs.org>.

## ■ AUTHOR INFORMATION

### Corresponding Author

\*E-mail: [djtantillo@ucdavis.edu](mailto:djtantillo@ucdavis.edu).

## Notes

The authors declare no competing financial interest.

## ■ ACKNOWLEDGMENTS

This work was supported in part by the U.S. National Science Foundation (CHE-0957416 and supercomputing resources through a grant from the XSEDE Program, CHE030089). We are grateful to Prof. K. N. Houk (UCLA) for sharing results on related systems prior to publication.

## ■ REFERENCES

- (1) Kelly, W. L. *Org. Biomol. Chem.* **2008**, *6*, 4483–4493.
- (2) Stocking, E. M.; Williams, R. M. *Angew. Chem., Int. Ed.* **2003**, *42*, 3078–3115.
- (3) Oikawa, H. *Bull. Chem. Soc. Jpn.* **2005**, *78*, 537–554.
- (4) Oikawa, H.; Tokiwano, T. *Nat. Prod. Rep.* **2004**, *21*, 321–352.
- (5) Pohnert, G. *ChemBioChem* **2001**, *12*, 873–875.
- (6) Roethle, P. A.; Hernandez, P. T.; Trauner, D. *Org. Lett.* **2006**, *8*, 5901–5904.
- (7) Tang, B.; Bray, C. D.; Pattenden, G. *Tetrahedron Lett.* **2006**, *47*, 6401–6404.
- (8) Wang, S. C.; Tantillo, D. J. *J. Org. Chem.* **2008**, *73*, 1516–1523.
- (9) Wang, G.; Liang, J.; Wang, Y.; Li, Q.; Ye, W. *J. Nat. Med.* **2008**, *6*, 251–253.
- (10) Wang, G.; Wang, Y.; Li, Q.; Liang, J.; Zhang, X.; Yao, X.; Ye, W. *Helv. Chim. Acta* **2008**, *91*, 1124–1129.
- (11) Zhao, B.; Wang, Y.; Zhang, D.; Jiang, R.; Wang, G.; Shi, J.; Huang, X.; Chen, W.; Che, C.; Ye, W. *Org. Lett.* **2011**, *13*, 3888–3891.
- (12) Zhao, B.; Wang, Y.; Zhang, D.; Huang, X.; Bai, L.; Yan, Y.; Chen, J.; Lu, T.; Wang, Y.; Zhang, Q. *Org. Lett.* **2012**, *14*, 3096–3099.
- (13) Wei, H.; Qiao, C.; Liu, G.; Yang, Z.; Li, C. *Angew. Chem., Int. Ed.* **2013**, *52*, 620–624.
- (14) All of the computations were carried out using the M06-2X method<sup>15</sup> as implemented in the Gaussian 09 software suite.<sup>16</sup> M06-2X has been applied previously to a variety of related reactions.<sup>17,18</sup> The nature of each optimized structure (minimum or transition state structure) was assessed via analysis of computed vibrational frequencies and, in some cases, intrinsic reaction coordinate (IRC) calculations.<sup>19,20</sup> Reported energies are free energies at room temperature. The gross effects of aqueous solvation were treated using the SMD continuum model (single-point energies).<sup>21</sup> Reported barriers for intermolecular reactions are based on energies of separate reactants. Structural drawings were created using Ball & Stick. Conformers for *ent*-virosaine A and virosaine B and the transition state structures leading to their formation were generated using the Spartan '10 software suite.<sup>23</sup>
- (15) Zhao, Y.; Truhlar, D. G. *Theor. Chem. Acc.* **2008**, *50*, 215–241.
- (16) Frisch, M. J.; et al. *Gaussian 09*, revision A.02; Gaussian, Inc.; Wallingford, CT, 2009.
- (17) Linder, M.; Brinck, T. *Phys. Chem. Chem. Phys.* **2013**, *15*, 5108–5114.
- (18) Krenske, E. H.; Agopcan, S.; Aviyente, V.; Houk, K. N.; Johnson, B. A.; Holmes, A. B. *J. Am. Chem. Soc.* **2012**, *134*, 12010–12015.
- (19) Gonzalez, C.; Schlegel, H. B. *J. Phys. Chem.* **1990**, *94*, 5523–5527.
- (20) Fukui, K. *Acc. Chem. Res.* **1981**, *14*, 363–368.
- (21) Marenich, A. V.; Cramer, C. J.; Truhlar, D. G. *J. Phys. Chem. B* **2009**, *113*, 6378–6396.
- (22) Müller, N.; Faulk, A.; Gsaller, G. *Ball & Stick Molecular Graphics, Application for MacOS Computers*, version 4.0a12; Johannes Kepler University: Linz, Austria, 2004.
- (23) Shao, Y.; et al. *Phys. Chem. Chem. Phys.* **2006**, *8*, 3172–3191.
- (24) Ess, D. H.; Houk, K. N. *J. Am. Chem. Soc.* **2007**, *129*, 10646–10647.
- (25) Ess, D. H.; Houk, K. N. *J. Am. Chem. Soc.* **2008**, *130*, 10187–10198.

- (26) Hayden, A. E.; Houk, K. N. *J. Am. Chem. Soc.* **2009**, *131*, 4084–4089.
- (27) Lopez, S. A.; Houk, K. N. *J. Org. Chem.* **2012**, *78*, 1778–1783.
- (28) van Zeist, W.; Bickelhaupt, F. M. *Org. Biomol. Chem.* **2010**, *8*, 3118–3127.
- (29) Fernández, I.; Bickelhaupt, F. M.; Cossío, F. P. *Chem.—Eur. J.* **2012**, *18*, 12395–12403.
- (30) Glendening, E. D.; Reed, A. E.; Carpenter, J. E.; Weinhold, F. *NBO 3.0*; University of Wisconsin, Madison, WI. This approach makes use of second-order perturbation theory.
- (31) After the original submission of this manuscript, a related study was published. See: Krenske, E. H.; Patel, A.; Houk, K. N. *J. Am. Chem. Soc.* **2013**, DOI: 10.1021/ja409928z.